

## 7.2 DISPERSION IN ATMOSPHERIC CONVECTIVE BOUNDARY LAYER WITH WIND SHEARS: FROM LABORATORY MODELS TO COMPLEX SIMULATION STUDIES

Evgeni Fedorovich\*

School of Meteorology, University of Oklahoma, Norman, Oklahoma

### 1. INTRODUCTION

Convective boundary layers (CBLs) driven by buoyancy forcings from the bottom or/and from the top and capped by temperature (density) inversions are commonly observed in the lower portion of earth's atmosphere (Holtslag and Duynkerke 1998). During fair-weather daytime conditions, the buoyancy forcing in the boundary layer is primarily represented by convective heat transfer from a warm underlying surface. Such buoyancy forcing generates up- and downward motions that effectively mix momentum and scalar fields inside the CBL. Due to active mixing, the wind velocity, potential temperature (buoyancy), and concentrations of atmospheric constituents in the main portion of the CBL (often referred to as convectively mixed layer) do not change considerably with height when averaged over horizontal planes or over time.

A typical CBL can be subdivided into three separate layers: the surface layer, in which the meteorological variables change fairly rapidly with height; the mixed layer, where mean vertical gradients of these variables close to zero; and the entrainment zone (also referred to as the inversion layer or interfacial layer), where again the large gradients in meteorological fields are observed. Across the entrainment zone, the free-atmosphere air, which is more buoyant than the CBL air, is entrained into the convectively mixed layer as the CBL grows. Such convective entrainment is maintained by the penetration of the thermals into the stably stratified atmosphere above the CBL and subsequent folding of more buoyant air from aloft into the CBL as these overshooting thermals sink back into the mixed layer.

Dispersion patterns in the atmospheric CBL are strongly variable both in time and in space. However, in the meteorological boundary-layer studies, two CBL types different with respect to their spatial-temporal evolution are usually considered. The first CBL type (we will call it the non-steady CBL) is (or assumed to be) statistically quasi-homogeneous over a horizontal plane. In this case, the CBL evolution is regarded as a non-stationary process. Most numerical and laboratory CBL studies reported in the literature have been carried out under the assumption of horizontal homogeneity of the layer. Available field measurement data on dispersion of

passive constituents in the CBL usually also refer to this CBL type. Another commonly studied case of the atmospheric CBL is the horizontally evolving CBL, which grows in a neutrally or stably stratified air mass that is advected over a heated underlying surface. This type of the CBL (we will call it the heterogeneous CBL) is a traditional subject of wind-tunnel model studies. Based on the Taylor hypothesis (Willis and Deardorff 1976b), it is generally possible to relate temporal and spatial scales of dispersive turbulent motions in the non-steady and heterogeneous CBLs (Fedorovich et al. 1996).

The turbulence structure and characteristics of dispersion in the atmospheric CBL have been rather thoroughly investigated for the case of non-steady CBL without wind shears (hereafter referred to as the case of shear-free CBL). Just a few studies have been devoted to the investigation of effects produced by additional non-convective (or non-buoyant) forcings that contribute to the CBL turbulence regime in conjunction with the dominant buoyant driving mechanism. Wind shear is an example of such forcing. In the developed CBL, the wind (momentum) field inside the layer is well mixed by convective motions and, as explained in Garratt et al. (1982), the flow regions with strong mean wind gradients (shears) are usually located at the surface (surface shear) and at the level of inversion (elevated shear).

Erich Plate was one of pioneers of wind tunnel studies of flow and dispersion in CBLs affected by wind shears. Laboratory experiments, conducted by him and his colleagues in the thermally stratified wind tunnel of the University of Karlsruhe (Germany) in the 1980-1990s, considerably contributed to our present understanding of dispersion processes in the sheared CBL and constituted an essential complementation to famous laboratory studies of dispersion in the shear-free water-tank CBL by Deardorff and Willis (1982, 1984) and Willis and Deardorff (1976a, 1978, 1981, 1983, 1987).

In the present paper, the growing complexity of investigated CBL dispersion phenomena and applied model approaches will be discussed in a historical retrospective. Recent results obtained in both non-steady and heterogeneous CBLs will be presented. The emphasis will be laid on the dispersion of non-buoyant plume of gaseous tracer emitted from a point source located at different elevations within the CBL.

### 2. LABORATORY MODELS OF CBL FLOWS

The pioneering laboratory studies of gaseous plume dispersion in the atmospheric CBL have been

---

\* *Corresponding author address:* Evgeni Fedorovich, School of Meteorology, University of Oklahoma, 100 East Boyd, Norman, OK 73019-1013; e-mail: fedorovich@ou.edu

performed in the 1970-1980s by Willis and Deardorff (1976a, 1978, 1981, 1983, 1987) and Deardorff and Willis (1982, 1984). In order to imitate a mean wind in the water-tank CBL, a model stack in the quoted experiments was towed along the bottom of the tank. Apparently, such technique only partially accounted for the effect of wind on the tracer dispersion. The mean advection of tracer was adequately reproduced in this case, while turbulent diffusive motions generated due to bottom friction and vertical shears were not taken into account. In an attempt to overcome this limitation of water-tank modeling techniques, an idea of composite water tank was later realized in the laboratory study of

Park et al. (2001). Their composite water tank system included a conventional water tank, similar to the one used in the experiments of Willis and Deardorff, and a moving grid plate for mechanical generation of turbulence near the bottom of the tank, which was intended to simulate the shear-produced turbulence. With mechanically generated turbulence, the authors of *op. cit.* managed to achieve rather close agreement between their laboratory data and CONDORS field experiment (Briggs 1993) results with respect to spatial variations of mean concentration pattern.

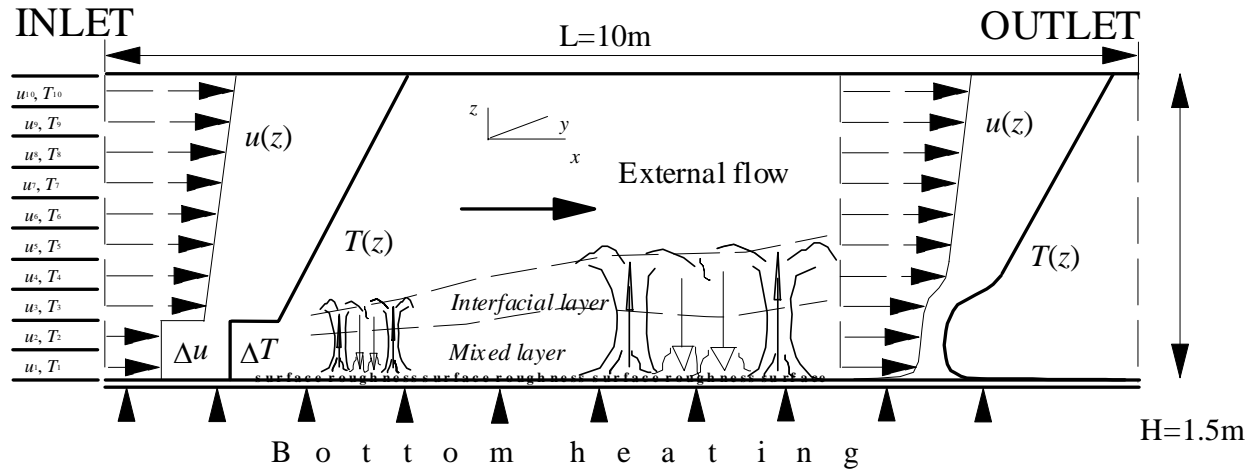


Figure 1. Sketch of horizontally evolving, sheared atmospheric CBL in the UniKa thermally stratified wind tunnel.

For interpretation of concentration distributions in the laboratory CBL, Willis and Deardorff applied the Deardorff (1970) convective (mixed-layer) scaling, further discussed in Deardorff (1985), which since that time has served as standard framework for inter-comparison of CBL dispersion data from different studies. This scaling has been originally proposed to normalize mean-flow parameters and turbulence statistics in the numerically simulated shear-free CBL. The scaling concept is based on three governing scales for length  $z_i$ , velocity  $w_*$ , and temperature  $T_*$ . The length scale  $z_i$  (interpreted as the CBL depth) is taken as the elevation the level of the most negative heat flux of entrainment within the interfacial layer, the velocity scale is related to  $z_i$  and to the surface kinematic heat flux  $Q_s$  as  $w_* = (\beta Q_s z_i)^{1/3}$ , where  $\beta = g/T_0$  is the buoyancy parameter ( $g$  is the acceleration due to the gravity,  $T_0$  is the reference temperature), and the temperature scale is defined through the ratio of  $Q_s$  to  $w_*$ :  $T_* = Q_s / w_*$ . For the purpose of normalization of concentration patterns in the CBL with mean wind, the above scaling was complemented with the horizontal

length scale  $L_h = (z_i \cdot U) / w_*$ , and the concentration scale  $C_* = E_s / (z_i^2 \cdot U)$ , where  $U$  is the mean wind velocity and  $E_s$  is the tracer source strength in units of volume per unit time (Deardorff 1985). Two other dimensionless parameters (numbers) based on the Deardorff (1970) convective scales are commonly employed to characterize turbulence regime in the CBL developing on the background of stable stratification (see e.g., Fedorovich et al. 1996): the Richardson number  $Ri_{\Delta T}$  related to the temperature increment  $\Delta T$  across the interfacial layer:  $Ri_{\Delta T} = \beta w_*^{-2} z_i \Delta T$ , and the Richardson number based on the buoyancy frequency  $N$  in the turbulence-free flow above the CBL:  $Ri_N = N^2 z_i^2 w_*^{-2}$ .

In their water tank experiments, Willis and Deardorff found that the source location was an important factor of the concentration distribution in the CBL. They have shown that the average centerline of the plume released from an elevated source in the CBL descended quickly downwind of the source. In contrast, the plume released near the surface rose fast inside the CBL. These observations, which were not consistent with predictions of the Gaussian plume model, manifested the specific character of dispersion in the CBL associated with the

skewed (narrow, fast updrafts versus broad, slow downdrafts) vertical velocity field.

Nevertheless, the discussed water-tank CBL model approaches either omitted or treated rather indirectly the effects of wind shears on the turbulence regime and characteristics of dispersion in the atmospheric CBL. With respect to taking these effects into account, the wind-tunnel modeling technique seems to be the most feasible one. A series of laboratory studies of plume dispersion in a sheared CBL have been conducted in specially designed thermally stratified wind tunnels in different countries of the world, see reviews by Meroney and Melbourne (1992) and Meroney (1998).

First wind-tunnel experiments of this kind have been carried out in the Colorado State University by Poreh and Cermak (1984). In their simulations, the floor of the first half of the test section was cooled to establish the stable stratification, which was eroded downstream, with the internal CBL growing over the heated second half of the floor. This method of CBL generation imposes serious limitations on a number of important integral parameters of the CBL, namely, the inversion strength, the boundary-layer depth, the temperature gradient in the turbulence-free layer, and the surface heat flux. The crucial problem of the cooling-heating approach is the necessity to have a very long test section in order to simulate a sufficiently deep CBL. However, Poreh and Cermak (1984) have measured parameters of the three-dimensional plume spread in the horizontally evolving CBL and found them to be in a fair qualitative agreement with atmospheric observations.



**Figure 2.** General view of the UniKa thermally stratified wind tunnel with insulated return section (upper part).

The first real opportunity to study in laboratory the effects of wind shears on dispersion in the CBL was presented in the late 1980s - early 1990s, when a thermally stratified wind tunnel was completed at the University of Karlsruhe (UniKa), Germany, under the scientific supervision of Erich Plate (Poreh et al. 1991, Rau et al. 1991, Rau and Plate 1995, Plate 1998). In the UniKa wind tunnel, the above mentioned shortcomings of the cooling-heating approach have been overcome by pre-shaping profiles of CBL mean-flow characteristics at the test-section inlet, see Fig. 1.

The UniKa tunnel is of the closed circuit type, with a test section 10 m long, 1.5 m wide and 1.5 m high. The floor of the test section, which is constructed of smooth aluminium plates, is heated, with energy input controlled to ensure a constant heat flux through the floor. The return section of the tunnel is subdivided into ten layers, which are individually insulated. Air flow in each 15-cm deep layer is driven by individual fan and heating system. By means of a feedback control system, disturbances in the flow are compensated while it passes through the return section, and steady-state inflow conditions are maintained within each layer. The two lower layers of the tunnel, of 0.3-m depth in total, operate in the open-circuit regime, with the incoming flow possessing the temperature of the ambient atmospheric air.

Shapes of the prescribed inlet profiles of velocity and temperature roughly correspond to their counterparts in the developed atmospheric CBL. The pre-shaped flow proceeds downstream over the heated floor of the tunnel, with convective turbulence penetrating into the flow and transforming it into the CBL-type flow. This revolutionary technique provides an opportunity to generate a deep CBL over a comparatively short fetch. By varying the initial temperature and velocity profiles, different forcings affecting the turbulence regime in the CBL can be investigated, for instance, effects of wind shears omitted in water-tank models of the CBL.



**Figure 3.** Interior of the UniKa thermally stratified wind tunnel. Winds in the insulated walls of the tunnel are used for laser Doppler flow measurements.

Characteristics of CBL flow simulated in the UniKa wind tunnel are comprehensively discussed in Fedorovich et al. (1996), Kaiser and Fedorovich (1998), and Fedorovich and Kaiser (1998). The conducted wind-tunnel experiments have shown that wind shears can essentially modify the turbulence dynamics in the CBL and parameters of turbulent exchange (entrainment) across the capping inversion. Later on, the wind-tunnel studies at UniKa have been complemented by numerical Large Eddy Simulation (LES) of the CBL flow reproduced in the tunnel (Fedorovich et al. 2001a,b; Fedorovich and Thäter 2001). This combination of numerical and laboratory approaches allowed a detailed

quantification of mean flow characteristics and turbulence statistics in the convectively driven flow modified by surface and elevated wind shears, see examples of flow statistics in Fig. 4.

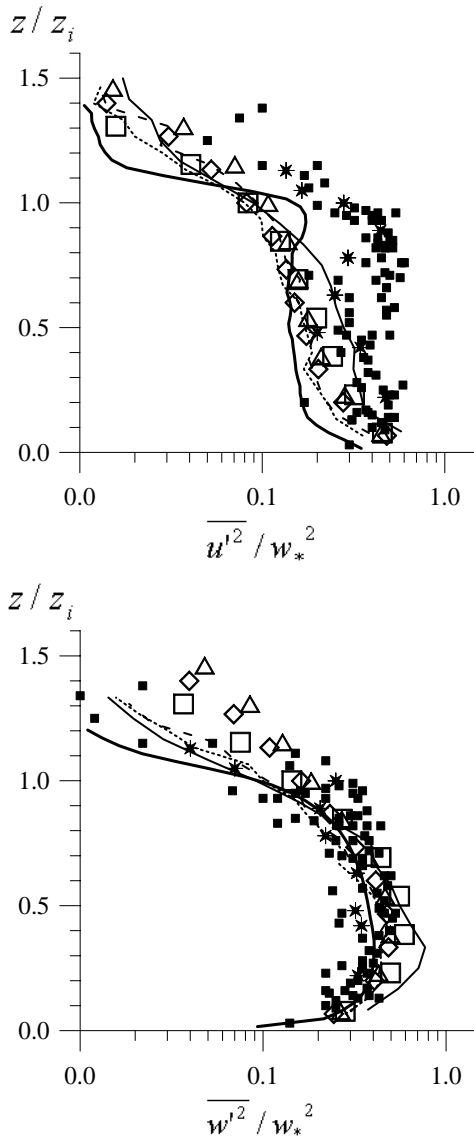


**Figure 4.** Longitudinal (upper plot) and vertical (lower plot) velocity variances in the quasi-homogeneous portion of the UniKa wind-tunnel CBL ( $x=3.98\text{m}$  - solid lines;  $x=5.63\text{m}$  - dashed lines, and  $x=7.28\text{m}$  - dotted lines) compared with data from other CBL studies. Numerical data of Fedorovich et al. (2001a) referring to the same locations in the tunnel are given by open squares, triangles, and diamonds, respectively. Shear-free CBL data from the LES of Schmidt and Schumann (1989, heavy solid lines) and water-tank model of Deardorff and Willis (1985, asterisks) are shown together with atmospheric data (filled squares) from Lenschow et al. (1980) and Caughey and Palmer (1979).

A number of wind-tunnel facilities capable of simulating the atmospheric CBL have been constructed during the two past decades in Japan. Recent CBL flow and dispersion experiments conducted in two of these facilities are described in Sada (1996) and Ohya et al. (1996, 1998). The tunnel used by the latter research team is, probably, the most technologically advanced facility among existing thermally stratified tunnels all over the world. It should be noted, however, that many ideas implemented in the design of this facility had originally been realized by Erich Plate and his colleagues in the design of the UniKa tunnel.

Sada (1996) studied tracer diffusion in a CBL with weak wind shear using the thermally stratified wind tunnel of Komae Research Laboratory. He found the Deardorff (1970) convective scaling to be applicable to the flow and diffusion patterns in the simulated CBL. The capping temperature inversion in the conducted wind-tunnel experiments was rather weak. That was a reason for substantial vertical spread of the plume in the upper portion of the wind-tunnel CBL. In the *op. cit.*, the experimentally obtained parameters of dispersion were not analyzed in conjunction with properties of turbulence in the simulated CBL, and effects of flow shear on the tracer dispersion in the CBL were not particularly investigated.

### 3. PLUME DISPERSION IN THE HORIZONTALLY EVOLVING CBL

Laboratory studies of plume dispersion were conducted in the UniKa wind-tunnel CBL model in 1996-2001 (Thäter et al. 2001, Fedorovich and Thäter 2002). They were complemented in 2000-2001 by numerical LES studies (Thäter et al. 2001, Fedorovich 2004).

The simulated CBL in the UniKa tunnel develops through several intermediate stages, which are described in Fedorovich et al. (2001a). The stage of quasi-homogeneous, slowly evolving CBL, which is the closest counterpart of the atmospheric CBL, is achieved at  $x \approx 5.5\text{m}$  downwind of the inlet. At this stage, the value of  $Ri_{\Delta T}$  in the wind-tunnel CBL model is about 10, which is generally smaller than typical  $Ri_{\Delta T}$  values in majority of numerical and water-tank CBL models. For most of cases studied in the tunnel, the value of friction velocity  $u_*$  was from 0.03 to 0.08 m/s and  $w_*$  - from 0.15 to 0.20 m/s, and thus the  $u/w_*$  ratios were within the range from 0.2 to 0.5, that is around the margin for surface to affect the CBL flow structure (Holtslag and Nieuwstadt 1986). For the diffusion experiments in the tunnel, a non-buoyant tracer gas ( $\text{SF}_6$ ) has been employed. The mixture of tracer gas with air was emitted in the central vertical plane of the tunnel at 3.32-m distance from the test-section inlet, close to the downwind edge of established CBL region. Concentration measurements have been made using standard technique based on the electron detector method. The measured concentration values have been averaged over two-minute time periods. For additional

information regarding the experimental setup see Fedorovich and Thäter (2002).

In Fig. 5, the longitudinal concentration distribution from a near-ground source in the sheared wind-tunnel CBL is plotted together with the concentration distribution from the Willis and Deardorff (1978) water-tank model of the shear-free CBL.

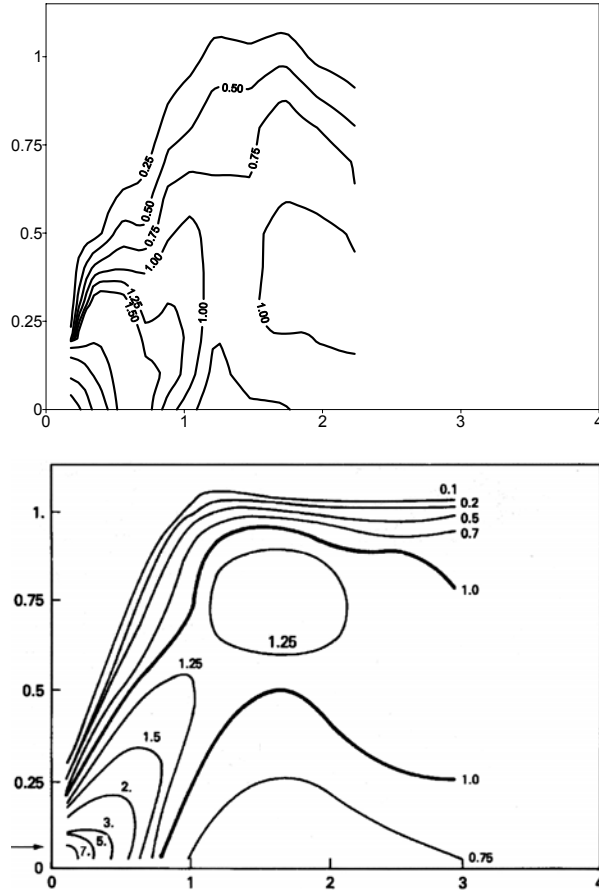


**Figure 5.** Dispersion of a non-buoyant plume in the water-tank model of shear-free CBL (Willis and Deardorff 1978, lower plot) and in the UniKa wind tunnel CBL (Fedorovich and Thäter 2002, upper plot). The source elevation is  $z/z_s=0.07$ . Height, length, and concentration are normalized by Deardorff (1970, 1985) convective scales. The origin of the x ordinate is at the source location.

From the qualitative point of view, the concentration distributions provided by both experimental techniques fairly agree with each other (one should keep in mind that the Taylor hypothesis was employed to enable comparability of the wind-tunnel distribution with the water-tank distribution). In both CBL models, the plume released near the surface rises fast inside the layer, which is a well-known feature of plume dispersion in the CBL (Lamb 1982). However, a closer inspection of the plots reveals the smaller horizontal concentration gradients in the lower portion of wind-tunnel CBL. This is apparently a result of enhanced longitudinal transport

of tracer by comparatively large horizontal velocity fluctuations associated with surface shear in the wind-tunnel flow.

In Fig. 6, a concentration distribution measured in the wind-tunnel CBL with imposed positive elevated shear (second plot from the top) is compared with its analog for the case of CBL with a shear-free upper interface (the uppermost plot).

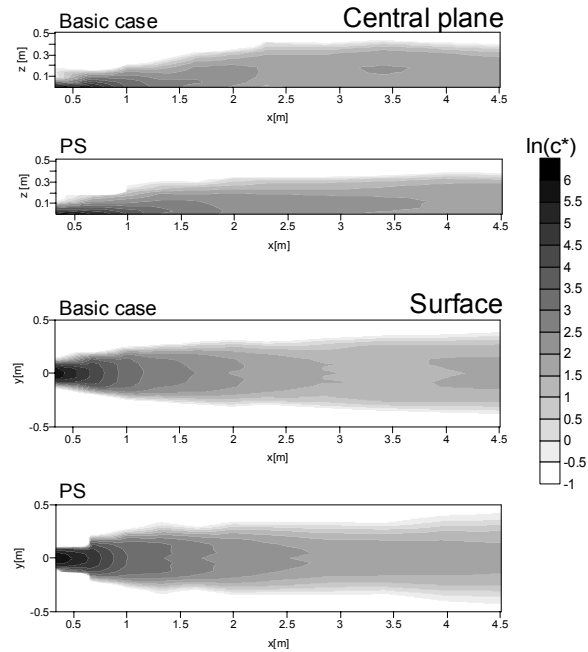


**Figure 6.** Longitudinal concentration distributions measured in the UniKa wind-tunnel CBL with positive elevated wind shear (PS) and in the basic CBL flow case without elevated shear (denoted as Basic case). The source is at the ground level in both cases. The origin of the x ordinate is at the source location. The capping-inversion and shear-zone elevations at  $x=0$  are 0.3 m.

Two upper concentration patterns refer to the central vertical plane of the tunnel. Concentration values in the plots are normalized as  $c_* = c \cdot L^2 \cdot U / E_s$ , where  $L=1\text{m}$ ,  $U=1\text{ m s}^{-1}$ . The presented comparison indicates that in the considered CBL case, the elevated positive shear amplifies the effect of stable stratification in obstructing the plume penetration above the inversion, which leads to a pronounced blocking of the tracer within the CBL. The resulting concentration levels at the same elevations along the wind-tunnel test section are noticeably smaller in the case of sheared inversion than in the CBL capped by a shear-free density interface. As one may also notice, the rise of the maximum concentration line in the case of sheared inversion is delayed in comparison with the reference shear-free case. The enhanced horizontal velocity fluctuations inside the sheared inversion lead to comparatively smooth horizontal distribution of concentration in the

upper portion of CBL with elevated shear (second plot from the top in Fig. 6).

In the CBL with positive elevated shear, the ground concentrations are generally higher than in the CBL flow with a shear-free inversion layer (compare two lower plots in Fig. 6). This is a result of accumulation of tracer in the congested and shallower boundary layer affected by the elevated wind shear.

Further results from the described wind-tunnel experiments, summarized in Fedorovich and Thäter (2002), indicate that the cross-stream concentration distribution in the sheared CBL displays features of plume channeling, which is presumably caused by longitudinal semi-organized roll-like motions in the CBL with shear.

A numerical study of dispersion in the UniKa wind-tunnel CBL was conducted by means of the LES code described Fedorovich et al. (2001a) with an added dispersion simulation module (Thäter et al. 2001). The Eulerian method considered in Nieuwstadt (1998) was employed for incorporation of the tracer transport in the LES framework, and the balance equation for the tracer concentration  $c$  was taken in the form:

$$\frac{\partial \bar{c}}{\partial t} + \frac{\partial (\bar{u}_i \cdot \bar{c})}{\partial x_i} = \frac{\partial}{\partial x_i} \left[ \mu_c \frac{\partial \bar{c}}{\partial x_i} - (\overline{cu_i} - \bar{c} \cdot \bar{u}_i) \right] + S_c,$$

where  $i=1, 2, 3$ ;  $t$  stands for the time,  $x_i = (x, y, z)$  are the right-hand Cartesian coordinates,  $\bar{u}_i = (\bar{u}, \bar{v}, \bar{w})$  are the resolved-scale components of the velocity vector,  $\bar{c}$  is the resolved-scale concentration of the tracer,  $S_c$  is the source term, and  $\mu_c$  is the molecular diffusivity of the tracer. The overbar signifies the grid-cell volume average. The quantities  $F_{si} = \overline{cu_i} - \bar{c} \cdot \bar{u}_i$  are the components of the subgrid concentration flux, respectively, which were parameterized as  $F_{si} = -K_c (\partial \bar{c} / \partial x_i)$ . The value of subgrid turbulent diffusivity  $K_c$  was assumed to be equal to the subgrid thermal diffusivity. The latter quantity was parameterized through the product of subgrid length scale and square root of the subgrid turbulence kinetic energy as described in Fedorovich et al. (2001a). Zero-gradient boundary conditions are employed for  $\bar{c}$  at the walls of simulation domain (the wind-tunnel test section), and the radiation condition was applied at the outlet. In the grid cell containing the source, the source term had the form:  $S_c = E_s / \Delta^3$ , where  $E_s$  is the source strength and  $\Delta^3 = \Delta x \Delta y \Delta z$  is the grid-cell volume. In all other grid cells of the simulation domain, the value of  $S_c$  was set equal to 0.

Numerically simulated concentration distributions for the basic CBL flow case with shear-free inversion and for the CBL with imposed positive elevated shear are presented in Fig. 7. There is an overall agreement between the measured (Fig. 6) and computed (Fig. 7) concentration distributions with respect to their integral

parameters. However, some important fine details of the tracer dispersion in the CBL such as plume-rise rate and surface concentration patchiness are rather poorly reproduced by the LES.

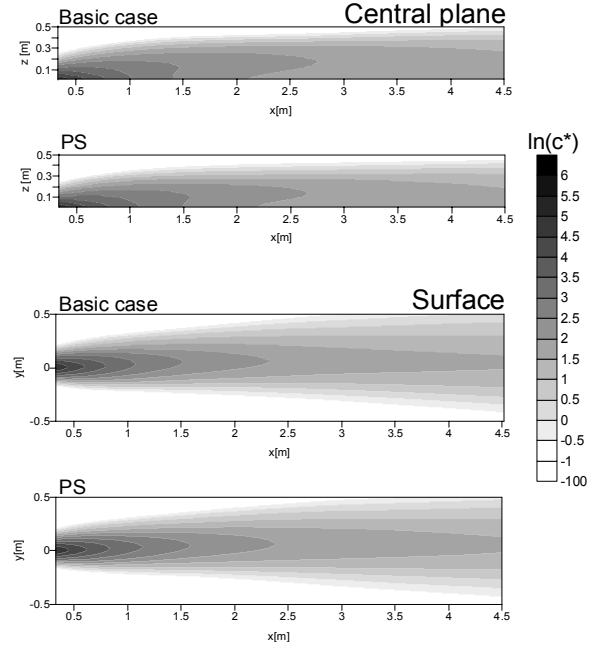


**Figure 7.** Longitudinal concentration distributions measured in the UniKa wind-tunnel CBL with positive elevated wind shear (PS) and in the basic CBL flow case without elevated shear (denoted as Basic case). The source is at the ground level in both cases. The origin of the  $x$  ordinate is at the source location. The capping-inversion and shear-zone elevations at  $x=0$  are 0.3 m.

The noted deficiencies are presumably due to insufficient spatial resolution of the conducted numerical simulations and spurious effects of the employed low-order advection scheme.

#### 4. PLUME DISPERSION IN THE NON-STEADY CBL WITH WIND SHEAR

A comprehensive numerical study of passive tracer dispersion in the non-steady, horizontally (quasi-) homogeneous CBL has been reported by Dosio et al. (2003). Following the Eulerian methodology, they added a conservation equation to the set of governing LES equations, previously employed for simulation of a variety of flow regimes in the atmospheric boundary layer. Similar methods to describe the tracer dispersion in the LES of CBL were previously used by Wyngaard and Brost (1984), Haren and Nieuwstadt (1989), Schumann (1989), and Henn and Sykes (1992). A different approach towards upgrading the LES for investigation of dispersion in the sheared CBL was exploited earlier by Mason (1992), who employed the Lagrangian framework to calculate the concentration patterns based on the LES-generated flow fields.

Wyngaard and Brost (1984) were first to demonstrate that properties of turbulent transport of the passive scalar emitted near the CBL bottom are rather different from the transport of a scalar emitted at the inversion level. This suggested bottom-up/top-down decomposition of diffusion offered a very useful framework for the analyses of dispersion patterns in the shear-free CBLs. However, the concept and associated scaling still await extension for the case of sheared CBL with both surface- and elevated-shear contributions to the diffusive turbulent motions.

Dosio et al. (2003) put numerical investigation of tracer dispersion in the CBL on a systematic basis and simulated dispersion regimes corresponding to four different values of geostrophic wind and three different values of surface heat flux in the simulation domain with a horizontal cross-section of 10km  $\times$  10km. The range of  $u_* / w_*$  in these numerical experiments was from 0.02 to 0.59. Thus, the CBL cases spanned in the study were from the practically shear-free CBL to the CBL with very significant contribution of surface shear to the turbulence production. Dispersion of tracer emitted from both the near-surface source ( $z_s / z_i = 0.078$ , where  $z_s$  is the source height) and the elevated source (placed almost in the middle of the CBL at  $z_s / z_i = 0.48$ ) was studied.

Results of the aforementioned numerical experiments for the CBL cases with  $u_* / w_*$  in the range from 0.02 to 0.21 have shown very good agreement with experimental data available from the laboratory (water-tank) and field studies of dispersion from a near-surface source in the weakly sheared CBL, see upper panels in Fig. 8. Presented plots demonstrate the comparison of the computed vertical,  $\sigma_z$  and  $\sigma_z'$ , and horizontal (lateral),  $\sigma_y$ , dispersion parameters with experimental data. These dispersion parameters were evaluated in the following way:

$$\sigma_z^2 = \frac{\int c(z - \bar{z})dV}{\int cdV}, \quad \sigma_z'^2 = \frac{\int c(z - z_s)dV}{\int cdV},$$

$$\sigma_y^2 = \frac{\int c(y - \bar{y})dV}{\int cdV},$$

where  $\bar{z}$  and  $\bar{y}$  are the mean plume height and the mean plume horizontal position, respectively. The dimensionless distance from the source,  $X$ , in the plots is defined based on the Deardorff (1970, 1985) convective scaling (see section 2).

At short distances from the source ( $X < 1$ ), the simulation results for  $\sigma_z'$  were found to fit well with the expression  $\sigma_z' / z_i = 0.52X^{6/5}$ , which is very close to the classical approximation  $\sigma_z' / z_i = 0.5X^{6/5}$  (Lamb 1982).

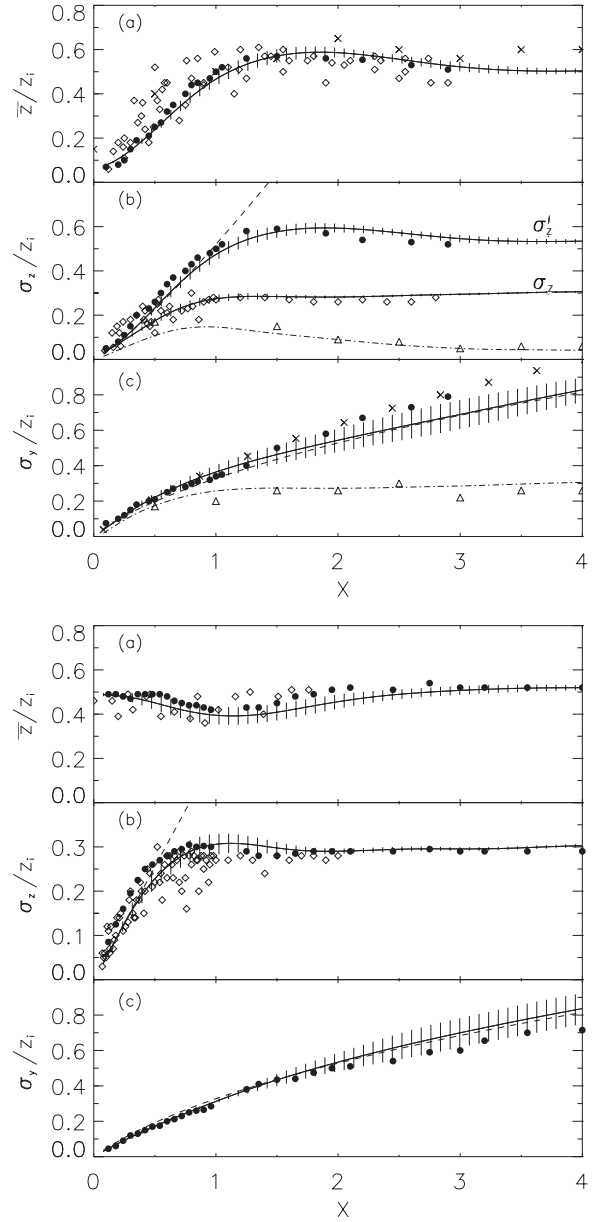


**Figure 8.** Horizontal changes of the plume height and dispersion parameters  $\sigma_z$ ,  $\sigma_z'$ , and  $\sigma_y$  in the practically shear-free ( $u_*/w_* \leq 0.21$ ) CBL with near-surface (upper panels) and elevated (lower panels) sources. The LES results of Dosio et al. (2003) are shown by solid lines with standard deviations indicated by vertical bars. Experimental data of Willis and Deardorff (1976), Weil et al. (2002), and Briggs (1993) are shown by filled circles,  $\times$  symbols, and diamonds, respectively. The dashed lines represent  $6/5$  and  $1$  power laws for  $\sigma_z'$  and  $\sigma_z$  (see explanations in the text), and the Gryning et al. (1987) parameterization for  $\sigma_y$ . The dashed-dotted line illustrates the simulated meandering component as compared with the water-tank data of Weil et al. (2002) shown by open triangles.

For the horizontal dispersion parameter  $\sigma_y$ , the LES results were in a good agreement with the laboratory data for  $X < 2$ . Besides that, they followed very closely the established analytical dependencies of  $\sigma_y/z_i$  on  $X$  discussed in the literature (Lamb 1982, Briggs 1985, and Gryning et al. 1987).

Rather satisfactory agreement was also found between the LES results and experimental data for the plume emitted from the elevated source (lower panels in Fig. 8). For the vertical plume dispersion, only  $\sigma_z$  values are shown in the plots because the mean plume height in this case does not noticeably deviate from the initial release height and thus  $\sigma_z' \approx \sigma_z$ . The power-law dependence on  $X$  for  $\sigma_z/z_i$  retrieved from the LES confirmed the parameterization suggested by Lamb (1982) for dispersion from elevated releases at  $X < 2/3$ :  $\sigma_z/z_i \approx 0.5X$ . The normalized lateral dispersion parameter  $\sigma_y/z_i$  as a function of  $X$  in the LES experiments with the elevated source followed approximately the same analytical curve as in the case of near-surface release, except for the region of small  $X$ , where the plume was spreading laterally slightly faster in the case of the near-surface release due to the enhanced horizontal fluctuations at the surface. This was found consistent with the unified parameterization suggested by Lamb for both releases at  $X > 1$ :  $\sigma_y/z_i \approx (1/3)X^{2/3}$ .

The LES results of Dosio et al. (2003) are of special interest with respect to quantification of the surface-shear effect on the dispersion of a plume emitted at different elevations within the CBL. In order to account for the shear in the normalized concentrations patterns, the authors of *op. cit.* used a modified velocity scale  $w_m$  introduced through the empirical formula  $w_m^3 = w_*^3 + 5u_*^3$  first suggested by Zeman and Tennekes (1977) for determination of velocity scale in the CBL with surface shear. The distance from the source  $x$  is then normalized as  $X_m = (w_m/z_i)(x/U)$ .

Numerical data presented in Fig. 9 (where upper panels show results for the near-surface release and lower panels refer to the elevated release) indicate that wind shear can considerably modify longitudinal variations of mean plume height and both vertical and lateral dispersion parameters in the CBL. The horizontal velocity fluctuations throughout a significant portion of the CBL are considerably enhanced by surface wind shear. These large fluctuations, in conjunction with the faster longitudinal transport of tracer by larger mean velocities, lead to relatively less effective vertical dispersion in the sheared CBL and, consequently, to the slower plume rise with distance and smaller values of the vertical dispersion parameter  $\sigma_z$ . At the same time, the lateral spread of the tracer in the sheared CBL is intensified by enhanced lateral velocity fluctuations, and the horizontal dispersion parameter  $\sigma_y$  grows with distance faster than in the case of shear-free CBL.

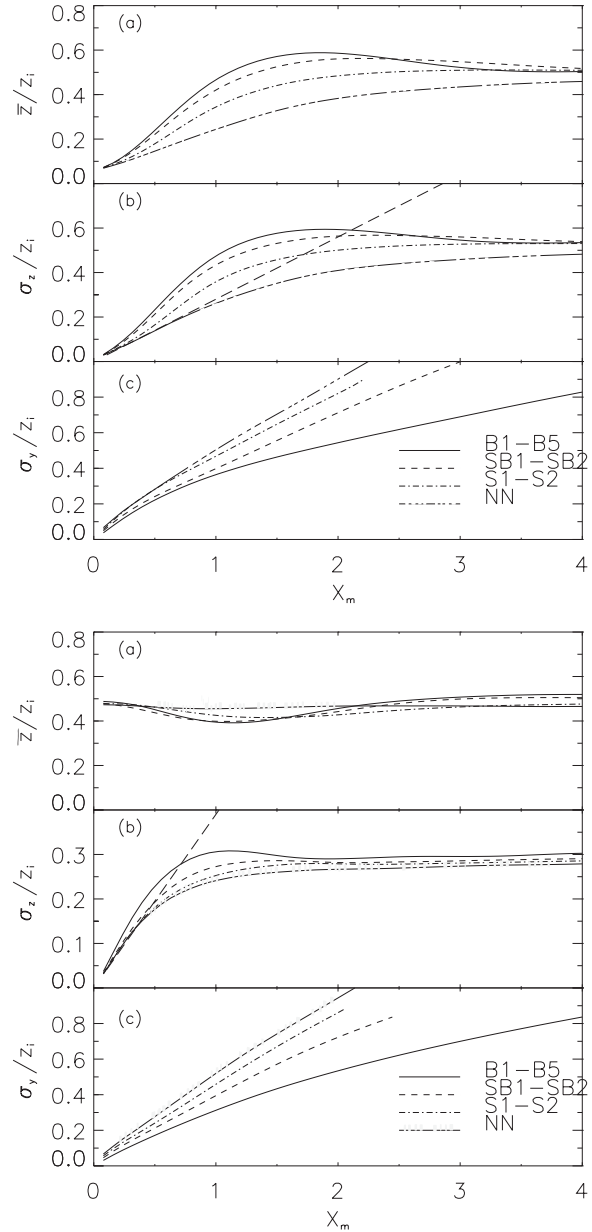


**Figure 9.** Effects of surface wind shear on the plume height and dispersion parameters  $\sigma_z$  and  $\sigma_y$  in the CBL with near-surface (left-hand panels) and elevated (right-hand panels) sources; from Dosio et al. (2003). The solid lines (cases B1-B5) show simulated parameters of the plume in the practically shear-free ( $u_*/w_* \leq 0.21$ ) CBL. The dashed lines (SB1-SB2) correspond to the CBL cases with moderate shear ( $u_*/w_* = 0.27$  and  $u_*/w_* = 0.34$ ). The dashed and dotted lines refer to the strongly-sheared CBL cases ( $u_*/w_* = 0.46$  and  $u_*/w_* = 0.47$ ). The case of nearly-neutral boundary layer (indicated as NN) is represented by  $u_*/w_* = 0.59$ .

The discussed shear effects on the plume of tracer released at the surface are perfectly illustrated by the



LES results shown in the upper panels of Fig. 9. Shear effects on dispersion in the CBL are generally less pronounced in the case of elevated release (lower panels in Fig. 9).

Based on their LES results, Dosio et al. (2003) concluded that the main effect of (surface) wind shear on the tracer dispersion in the atmospheric CBL is represented by a reduction of the vertical spread of a tracer, whereas its horizontal spread is enhanced. Consequently, the ground concentrations are strongly influenced as the increased wind tends to advect the plume for a longer time. The tracer, therefore, reaches the ground at greater distances from the source.

## 5. CONCLUDING REMARKS

The state-of-the-art laboratory and numerical model approaches towards the description of dispersion processes in the atmospheric convective boundary layer with surface and elevated wind shears have been considered in a historical prospective. In the review of numerical techniques, emphasis was laid on the Large Eddy Simulation (LES) of dispersion. In modern atmospheric dispersion studies, LES is primarily used as a scientific tool. However, one may expect that with growing computer power, this simulation technique will be employed more frequently as an applied research tool.

The reviewed results of laboratory and numerical studies have indicated that wind shears can have a significant impact on various characteristics of dispersion in the CBL. The plume height, ground-level concentration, vertical and horizontal dispersion parameters, and crosswind-integrated concentrations in the CBL are all noticeably affected by wind shears. The continued development of LES and the forthcoming implementation of Direct Numerical Simulation (DNS), which seems to be not very remote, in the studies of atmospheric dispersion on surface- and boundary-layer scales, will provide researchers with data about more detailed dispersion parameters such as concentration fluxes, variances, and higher-order statistics.

The analyses and interpretations of these new numerical data will never be conclusive and complete without new laboratory and field experimental data available for verification of numerical simulations. Unfortunately, I am not aware of any new field campaigns planned to study fine features of plume dispersion in the atmospheric CBL with wind shears. Laboratory studies of dispersion are, regretfully, also losing ground due to their high costs and non-attractiveness to scientists of younger generation, who tend to seek primarily numerical solutions to atmospheric problems. In this sense, the progress of boundary-layer dispersion studies crucially depends on the readiness of the scientific community, and society in general, to invest money and effort in the adequate experimental facilities, both laboratory and full-scale.

**Acknowledgement:** The author gratefully acknowledges support by the National Science Foundation (grant ATM-0124068).

- Briggs, G. A., 1985: Analytical parameterization of diffusion: the convective boundary layer. *J. Climate Appl. Meteor.*, **24**, 1167-1186.
- , 1993: Plume dispersion in the convective boundary layer. Part II: Analyses of CONDORS field experiment data. *J. Appl. Meteor.*, **32**, 1388-1425.
- Caughey, S. J. and Palmer, S. G., 1979: Some aspects of turbulence structure through the depth of the convective boundary layer, *Quart. J. Roy. Meteor. Soc.*, **105**, 811-827.
- Dearhoff, J. W., 1970: Convective velocity and temperature scales for the unstable planetary boundary layer and for Raleigh convection. *J. Atmos. Sci.*, **27**, 1211-1213.
- , 1985: Laboratory experiments on diffusion: the use of convective mixed-layer scaling. *J. Climate Appl. Meteorol.*, **24**, 1143-1151.
- , and G. E. Willis, 1982: Ground-level concentrations due to fumigation into an entraining mixed layer. *Atmos. Environ.*, **16**, 1159-1170.
- , and G. E. Willis, 1984: Ground-level concentration fluctuations from a buoyant and non-buoyant source within a laboratory convectively mixed layer. *Atmos. Environ.*, **18**, 1297-1309.
- , and G. E. Willis, 1985: Further results from a laboratory model of the convective planetary boundary layer. *Bound.-Layer Meteor.*, **32**, 205-236.
- Dosio A., J. Vilà-Guerau de Arellano, A. A. M. Holtslag, and P. J. H. Builtjes, 2003: Dispersion of a passive tracer in buoyancy- and shear-driven boundary layer. *J. Appl. Meteor.*, **42**, 1116-1130.
- Fedorovich, E., 2004: Dispersion of passive tracer in the atmospheric convective boundary layer with wind shears: a review of laboratory and numerical model studies. *Meteorol. Atmos. Phys.*, DOI: 10.1007/s00703-003-0058-3.
- , R. Kaiser, M. Rau, and E. Plate, 1996: Wind-tunnel study of turbulent flow structure in the convective boundary layer capped by a temperature inversion. *J. Atmos. Sci.*, **53**, 1273-1289.
- , and R. Kaiser, 1998: Wind tunnel model study of turbulence regime in the atmospheric convective boundary layer. *Buoyant Convection in Geophysical Flows*, E. J. Plate et al., Eds., Kluwer, 327-370.
- , F. T. M. Nieuwstadt, and R. Kaiser, 2001a: Numerical and laboratory study of horizontally evolving convective boundary layer. Part I: Transition regimes and development of the mixed layer. *J. Atmos. Sci.*, **58**, 70-86.
- , F. T. M. Nieuwstadt, and R. Kaiser, 2001b: Numerical and laboratory study of horizontally evolving convective boundary layer. Part II: Effects of elevated wind shear and surface roughness. *J. Atmos. Sci.*, **58**, 546-560.
- , and J. Thäter, 2001: Vertical transport of heat and momentum across a sheared density interface at the top of a horizontally evolving convective boundary layer. *Journal of Turbulence*, **2**, 007.

- , and J. Thäter, 2002: A wind tunnel study of gaseous tracer dispersion in the convective boundary layer capped by a temperature inversion. *Atmos. Environ.*, **36**, 2245-2255.
- Garratt, J. R., J. C. Wyngaard, and R. J. Francey, 1982: Winds in the atmospheric boundary layer: prediction and observation. *J. Atmos. Sci.*, **39**, 1307-1316.
- Gryning, S.-E., A. A. M. Holtslag, J. S. Irwin, and B. Siversten, 1987: Applied dispersion modeling based on meteorological scaling parameters. *Atmos. Environ.*, **21**, 79-89.
- Haren, L. van, and F. T. M. Nieuwstadt, 1989: The behavior of passive and buoyant plumes in a convective boundary layer, as simulated with a large-eddy model. *J. Appl. Meteor.*, **28**, 818-832.
- Henn, D. S., and S. R. Sykes, 1992: Large-eddy simulation of dispersion in the convective boundary layer. *Atmos. Environ.*, **26A**, 3145-3159.
- Holtslag A. A. M, and P. G. Duynkerke, Eds., 1998: *Clear and Cloudy Boundary Layers*. Royal Netherlands Academy of Arts and Sciences, Amsterdam, 372 pp.
- , and F. T. M. Nieuwstadt, 1986: Scaling the atmospheric boundary layer. *Bound.-Layer Meteor.*, **36**, 201-209.
- Kaiser, R., and E. Fedorovich, 1998: Turbulence spectra and dissipation rates in a wind tunnel model of the atmospheric convective boundary layer. *J. Atmos. Sci.*, **55**, 580-594.
- Lamb, R. G., 1982: Diffusion in the convective boundary layer. *Atmospheric Turbulence and Air Pollution Modelling*, F. T. M. Nieuwstadt and H. van Dop, Eds., D. Reidel, Dordrecht, 159-229.
- Lenschow, D. H., J. C. Wyngaard, and W. T. Pennel, 1980: Mean-field and second-momentum budgets in a baroclinic, convective boundary layer. *J. Atmos. Sci.*, **37**, 1313-1326.
- Mason, P. J., 1992: Large-eddy simulation of dispersion in convective boundary layers with wind shear. *Atmos. Environ.*, **26A**, 1561-1571.
- Meroney, R. N., 1998: Wind tunnel simulation of convective boundary layer phenomena: simulation criteria and operating ranges of laboratory facilities. *Buoyant Convection in Geophysical Flows*, E. J. Plate et al., Eds., Kluwer, 313-326.
- Meroney, R. N., and W. H. Melbourne, 1992: Operating ranges of meteorological wind tunnels for the simulation of convective boundary layer (CBL) phenomena. *Bound.-Layer Meteor.*, **61**, 145-174.
- Ohya, Y., K. Hayashi, S. Mitsue, and K. Managi, 1998: Wind tunnel study of convective boundary layer capped by a strong inversion. *J. Wind Engineering*, **75**, 25-30.
- , M. Tatuno, Y. Nakamura, and H. Ueda, 1996: A thermally stratified boundary layer tunnel for environmental flow studies. *Atmos. Environ.*, **30**, 2881-2887.
- Park, O. H., S. J. Seo, and S. H. Lee, 2001: Laboratory simulation of vertical plume dispersion within a convective boundary layer. *Bound.-Layer Meteor.*, **99**, 159-169.
- Plate E. J., 1998: Convective boundary layer: a historical introduction. *Buoyant Convection in Geophysical Flows*, E. J. Plate et al., Eds., Kluwer, 1-22.
- Poreh, M., and J. E. Cermak, 1984: Wind tunnel simulation of diffusion in a convective boundary layer. *Bound. Layer Meteorol.*, **30**, 431-455.
- , M. Rau and E. Plate, 1991: Design considerations for wind tunnel simulations of diffusion within the convective boundary layer. *Atmos. Environ.*, **25A**, 1250-1257.
- Rau, M., W. Bächlin and E. Plate, 1991: Detailed design features of a new wind tunnel for studying the effects of thermal stratification. *Atmos. Environ.*, **25A**, 1258-1263.
- Rau, M., and E. Plate, 1995: Wind tunnel modelling of convective boundary layers. *Wind Climate in Cities*, J. Cermak et al., Eds., Kluwer, 431-456.
- Sada, K., Wind tunnel experiment on convective planetary boundary layer, 1996: *J. Japan Soc. Mech. Eng.*, **58**, 3677-3684.
- Schmidt, H., and U. Schumann, 1989: Coherent structure of the convective boundary layer derived from large-eddy simulations. *J. Fluid. Mech.*, **200**, 511-562.
- Schumann U., 1989: Large-eddy simulation of turbulent diffusion with chemical reactions in the convective boundary layer. *Atmos. Environ.*, **23**, 1713-1727.
- Thäter, J., E. Fedorovich, and G. Jirka, 2001: A combined numerical and laboratory study of dispersion from a point source in the atmospheric convective boundary layer with wind shear. *Proc. Third Intern. Symp. on Environmental Hydraulics (ISEH2001)*, 5-8 December 2001, Tempe, Arizona, USA, 6 pp. (*ISEH2001 Abstracts*, 133-134).
- Venkatram, A., 1988: Dispersion in the stable boundary layer. *Lectures on Air Pollution Modeling*, A. Venkatram and J. C. Wyngaard, Eds., American Meteorological Society, 228-265.
- Weil, J. C., W. H. Snyder, R. E. Lawson, Jr., M. S. Shipman, 2002: Experiments on buoyant plume dispersion in a laboratory convection tank. *Bound.-Layer Meteor.*, **102**, 367-414.
- Willis, G. E., and J. W. Deardorff, 1976a: A laboratory model of diffusion into the convective boundary layer. *Quart. J. R. Met. Soc.*, **102**, 727-745.
- , and J. W. Deardorff, 1976b: On the use of Taylor's translation hypothesis for diffusion in the mixed layer. *Quart. J. Roy. Meteor. Soc.*, **102**, 817-822.
- , and J. W. Deardorff, 1978: A laboratory study of dispersion from an elevated source within a modeled convective planetary boundary layer. *Atmos. Environ.*, **12**, 1305-1311.
- , and J. W. Deardorff, 1981: A laboratory study of dispersion from a source in the middle of the convectively mixed layer. *Atmos. Environ.*, **15**, 109-117.
- , and J. W. Deardorff, 1983: On plume rise within a convective boundary layer. *Atmos. Environ.*, **17**, 2435-2447.
- , and J. W. Deardorff, 1987: Buoyant plume dispersion and inversion entrapment in and above a

laboratory mixed layer. *Atmos. Environ.*, **21**, 1725-1735.

Wyngaard, J. C. and R. A. Brost, 1984: Top-down and bottom-up diffusion of a scalar in the convective boundary layer. *J. Atmos. Sci.*, **41**, 102-112.